Sub-10^{-16} Frequency Stability in Multi-Pole Linear Ion Trap Standards: Reduction of Number-Dependent Sensitivity

E. A. Burt[1] and R. L. Tjoelker[1]

The JPL multi-pole linear ion trap standard (LITS) has demonstrated excellent frequency stability and improved immunity from two of its remaining systematic effects, the second-order Doppler shift and second-order Zeeman shift. In this article, we report developments that reduce the residual systematic effects to less than 6×10^{-17}. *We also report a new mode of operation that enables improved short-term stability to less than* $4 \times 10^{-14}/\tau^{1/2}$, *and the highest ratio of atomic transition frequency to frequency width (atomic line Q) ever demonstrated in a microwave atomic standard operating at room temperature. With these advances, the multi-pole LITS provides a new and unique timekeeping and reference capability in the JPL Frequency Standards Test Laboratory, with broader applicability to national metrology and timekeeping laboratories.*

I. Introduction

Continuously running frequency standards with state-of-the-art frequency stability are required for timekeeping and deep-space tracking applications. Doppler spacecraft tracking, very long baseline interferometry (VLBI), and radio science activities require high frequency and time stability to accurately locate and direct spacecraft, precisely time send and receive signals, or to correlate signals received in different locations. Linear ion trap standards (LITSs) developed at the Jet Propulsion Laboratory (JPL) have demonstrated excellent short- [1,2] and long-term stability [3] and also have demonstrated long-term field operation. The relative insensitivity to the second-order Doppler shift using a multi-pole linear ion trap configuration [4] has resulted in a mercury ion (Hg^+) frequency standard with excellent long-term stability [5]. Even further reduction of the primary multi-pole LITS systematic sensitivities, which are already small, is the main focus of this article. This advanced multi-pole LITS provides a new capability for timekeeping and serves as an unambiguous performance reference of other very stable atomic standards and global time and frequency transfer methods.

The multi-pole LITS operates continually at room temperature and requires no laser or microwave cavity. The exceptional performance has been realized even though it currently has no feedback control of the three largest remaining systematic effects: (1) variations in the number of ions trapped, (2) variations in the (shielded) ambient magnetic field, and (3) variations in background pressure. The combined

[1] Tracking Systems and Applications Section.

The research described in this publication was carried out by the Jet Propulsion Laboratory, California Institute of Technology, under a contract with the National Aeronautics and Space Administration.

contribution of these effects to the long-term fractional frequency instability of the multi-pole LITS has already been measured at $<2 \times 10^{-16}$/day [5]. Although the multi-pole LITS frequency already has low sensitivity to the number of ions trapped, this remains the largest contributing factor to small frequency variations observed over the long term.

The number-dependent shift was first characterized [6] with initial operation of the multi-pole LITS. Although the sensitivity was low, the shift had the opposite sign of that expected for a second-order Doppler shift. This anomalous shift has since been demonstrated to be a number-dependent effect consisting of a combination of the ion-number-dependent second-order Doppler shift and a small contribution due to magnetic field inhomogeneity [7]. Although ultimately it may be beneficial to place the ion number in a control loop, an essential first step is to reduce the sensitivity of the standard to ion-number-dependent shifts as much as possible. In this article, we present a thorough characterization of the number-dependent effect and a demonstrated method for further reducing it.

The next largest sensitivity in the multi-pole LITS is the buffer-gas-induced pressure shift. In this article, we describe a new buffer-gas system consisting of a neon capillary leak. Neon has a smaller frequency shift in Hg^+ than does the previous buffer gas, helium, and less of it is required to achieve the same cooling.

II. Multi-Pole LITS Configuration

The $^{199}Hg^+$ LITS is designed for continuous operation and with components that can operate for months to years without intervention. For example, the LITS uses no lasers, but instead uses a $^{202}Hg^+$ plasma discharge lamp for state preparation and read out and a noble buffer gas for ion cooling.

The multi-pole ion trap has been described in detail elsewhere [4,8]. The physics package consists of a quadrupole trap, similar to those used in the predecessor LITS, that is used for the initial ion loading and state preparation. The ions are held near room temperature, typically via collisions with a helium buffer gas with a partial pressure of about 10^{-5} torr. The present multi-pole trap consists of 12 rods and is an extension of the quadrupole loading trap (Fig. 1). Ions are "shuttled" between the two traps by varying their relative DC bias potentials, with loading taking place in the quadrupole trap and the sensitive microwave interrogation taking place in the separate multi-pole trap. As derived in [4,8], a key

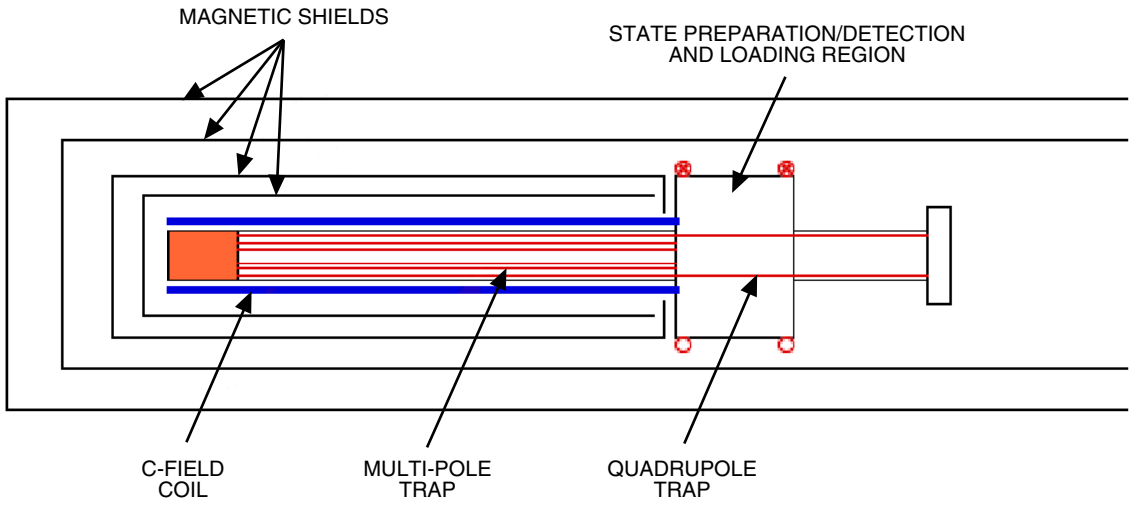

Fig. 1. The multi-pole LITS physics package. Shown is a schematic of the relative positions of key components (not to scale).

feature of the multi-pole trap is that the average radio frequency (RF) amplitude experienced by the ion cloud is smaller than in the corresponding quadrupole trap, resulting in a smaller second-order Doppler shift. Another benefit is that microwave interrogation of the ions takes place in an improved magnetic environment located well away from contact potentials and stray light that could be present in the ion-loading and state-preparation trap. Microwaves to interrogate the 40.5-GHz ground-state hyperfine transition are delivered to the multi-pole trap using a ceramic waveguide inside the vacuum enclosure.

Two multi-pole LITSs have been developed at JPL, identified as LITS-8 and LITS-9. LITS-8 was installed at the U.S. Naval Observatory (USNO) and has been operating there since 2002 [5]. With the completion of this enhanced capability, LITS-9 is now operating at the JPL Frequency Standards Test Laboratory. Both LITS-8 and LITS-9 are optimized for long-term continuous operation and timekeeping applications. Smaller standards using the multi-pole trap configuration are also being developed at JPL for spaceflight applications [9–11]. A very small physics unit has recently been constructed using a sealed vacuum system showing an excellent signal-to-noise ratio (SNR) [12].

III. Multi-Pole LITS Performance

The multi-pole LITS has demonstrated a short-term performance as low as $7\times10^{-14}/\tau^{1/2}$ and reference maser limited long-term performance. Over a 9-month period, LITS-8, operating in the clock ensemble at USNO, has not deviated in fractional frequency from the USNO master clock by more than 2×10^{-14} or shown a fractional frequency drift of more than 2×10^{-16}/day [5]. While this is excellent performance, in this article we identify the source of this residual drift and the method to further reduce it.

A. Multi-Pole LITS Systematics

Table 1 lists known systematic shifts or limits associated with the $^{199}Hg^{+}$ multi-pole LITS-8. The helium pressure shift assumes a background partial pressure of 10^{-5} torr of helium. Pressure shifts for other gas species assume partial pressures of less than 10^{-9} torr. The light shift estimate assumes a lamp output (dim state) of 100 μW/cm^2 with a 1-GHz spectral width offset 3 GHz from the 194-nm, 6s $^2S_{1/2}$–6p $^2P_{1/2}$ optical transition, and an ion temperature of 500 K. The estimate also assumes that light reflected from the loading region into the sensitive interrogation region is attenuated by more than 10^4. A C-field of 80 mG is used for Zeeman calculations. The RF AC Zeeman and Stark shifts assume a 1-MHz RF amplitude of 35 V. The stability floor for the second-order Doppler shift is an upper bound since it

Table 1. Systematic fractional frequency shifts for the $S_{1/2}\,F=0, m_F=0 - S_{1/2}\,F=1, m_F=0$ microwave clock transition in the multi-pole Hg^{+} LITS.

Shift	Scaling	Magnitude	Systematic floor
Second-order Doppler shift–multi-pole trap [8]	$-\langle v^2/c^2\rangle$	-1×10^{-13}	$<5\times10^{-16}$
He pressure shift [13,14]	$P_{\rm He}$	3×10^{-13}	$<2\times10^{-16}$
Hg pressure shift	$P_{\rm Hg}$	Unknown	$<2\times10^{-16}$
Other pressure shifts (H, N, CO, CO_2, CH_4, etc.) [14]	$P_{\rm other}$	$<10^{-16}$	$<10^{-16}$
194-nm light shift (estimate)	I_{194}	2×10^{-16}	2×10^{-17}
Second-order Zeeman shift [7]	$\langle B^2\rangle$	1.5×10^{-11}	1.5×10^{-17}
Black-body shift [15]	$-T^4_{\rm ambient}$	-1×10^{-16}	1.3×10^{-19}
RF AC Zeeman shift	$\langle B^2_{\rm rf}\rangle$	$<2\times10^{-13}$	$<2\times10^{-19}$
RF AC Stark shift [15]	$\langle E^2_{\rm rf}\rangle$	$<10^{-19}$	$<10^{-19}$

probably includes other indirect sensitivities (such as to helium pressure stability). Previous versions of the LITS used helium as a buffer gas. The helium pressure shift is the next largest systematic effect. To reduce sensitivity to buffer-gas pressure fluctuations, LITS-9 now uses neon as the buffer gas.

IV. Ion-Number-Dependent Effects

Previously, the LITS second-order Doppler shift effect has been characterized by varying the trapped number of ions. However, there are three ways that varying the ion number can affect the LITS clock frequency. The second-order Doppler shift in an ion trap has two components: one due to the temperature of the ions, which is indirectly related to the ion number, and the other due to geometric effects that are exacerbated by trapped ion number changes. For the second component, as ion number is increased, space charge repulsion causes the ion cloud volume to increase, thereby increasing the average RF trap amplitude experienced by the ions. The amplitude of the ion micro-motion is proportional to the RF trap potential, hence a number-dependent second-order Doppler shift. Since this effect scales with $-\langle v^2/c^2 \rangle$, a second-order Doppler shift has a negative slope when plotted against an increasing ion number. This effect is greatly reduced in a multi-pole trap because the trap potential approximates a square well and the average RF amplitude experienced by the ions is much smaller than in a quadrupole trap. A third ion number effect is magnetic in origin. Great care is taken in the multi-pole LITS to create a uniform C-field with a solenoid. Unfortunately, due to the finite solenoid length, some fringing in the field exists at the ends, which overlap the trap volume. As the ion number is increased, the ion cloud volume increases and now experiences a different value of $\langle B^2 \rangle$, where the average is taken over the ion cloud volume, as shown schematically in Fig. 2.

Due to fringing, $\langle B^2 \rangle$ decreases with ion cloud volume and, therefore, with ion number as well, leading to a decreasing second-order Zeeman shift. In this case, the slope of the shift when plotted against ion number is negative, as with the number-dependent second-order Doppler shift. However, the ends of the solenoid are also very close to the end caps of the inner two magnetic shield layers, which can cause a slight field increase. If the field increases near the solenoid ends, then the slope of the magnetic inhomogeneity effect will be positive. Thus, the combination of the number-dependent second-order Doppler shift and the number-dependent second-order Zeeman shift can lead to either a positive or negative slope for the frequency shift as a function of ion number. The number-dependent effect in the multi-pole LITS has been previously correlated with changes in the average magnetic field using the field-sensitive $m = 0$ to $m = \pm 1$ transitions [4].

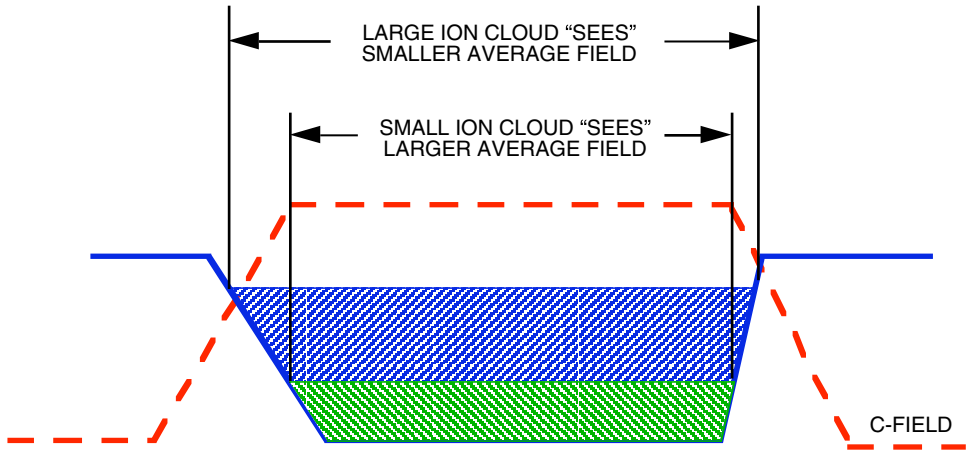

Fig. 2. A cross section of the trap potential in the axial direction superimposed with a C-field that has fringing at the ends. As the ion cloud volume increases, the value of $\langle B^2 \rangle$ decreases, and so does the ion-number-dependent shift. The effect is conceptually similar, though smaller, in the radial direction.

A. Ion-Number Dependence in LITS-8

The method used most often to vary the number of trapped ions is to change the trapping potentials, typically the end cap DC bias voltage for the load trap. While this does vary the ion number, it also impacts other ion cloud characteristics, such as temperature. To rule out the possibility of another systematic effect "masquerading" as an ion-number-dependent effect, it is useful to have an orthogonal way of varying ion number. One approach is to vary the temperature of the mercury oven, but the time required to reach equilibrium is long and this approach is generally not used. However, recently the LITS-8 mercury source was replenished at the USNO. The mercury oven temperature was subsequently increased in several steps over a 6-month period. During this time, the LITS-8 frequency offset was monitored, allowing this orthogonal measurement of ion-number dependence. Figure 3 shows the clock resonance signal size and frequency offset plotted on the same graph.

The total frequency shift for the data shown in Fig. 3 from an empty to full trap is about 3 mHz or a fractional frequency shift of about 7.5×10^{-14}, which is the same as found by varying the load trap potential. The correlation between the frequency offset and changes in signal size (due to discrete changes in the mercury oven temperature that are not part of normal clock operation), which is assumed proportional to ion number, is evident. This implies that most of the frequency deviation from the USNO master clock observed previously is due to this effect. Insofar as we are able to mitigate ion-number dependence, we are likely to improve stability by equal measure.

One notable event where the correlation does not hold occurs at day 160. Here the signal size makes a discrete jump while the frequency remains stable. Clock telemetry for this time period shows that the total light level (signal size plus background) changed by more than the drop in signal size alone, indicating a change in the lamp output. Changes in lamp state are not uncommon, and the frequency algorithm is immune to lamp-output variations to second order. We conclude that the lack of correlation at this one point is due to a lamp-state change and not an ion-number change.

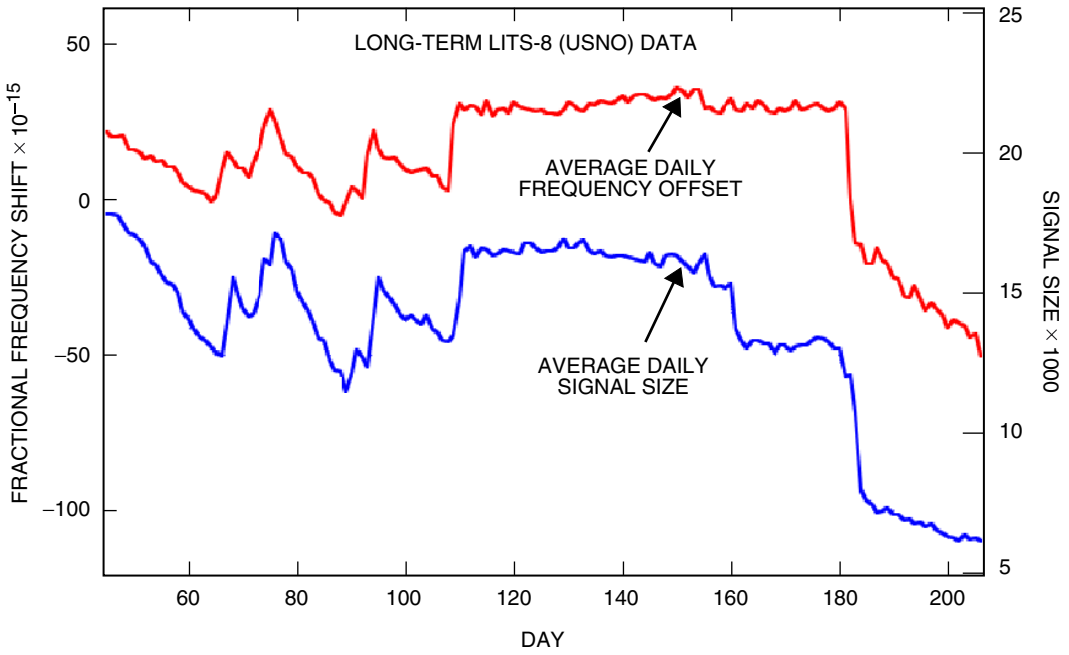

Fig. 3. Fractional frequency shift and signal size data for LITS-8 over a 6-month period from November 2004 to May 2005. Frequency offsets are measured from an H-maser referenced to the USNO master clock. Signal size is assumed to be proportional to trapped ion number. Jumps in the signal size before day 120 were due to discrete changes in the mercury oven temperature. The signal size change at day 180 was due to an electronic problem that reduced the trapping potential. The change in signal size at day 160 that does not correlate with a frequency change is explained in the text.

V. Modeling Ion-Number Dependence

Having verified that the long-term frequency stability is affected by changes in ion number and suspecting that the sensitivity has a magnetic component, we turn to modeling the effect of magnetic-field inhomogeneity in the multi-pole region of the physics package. The trap, solenoid, and shields have azimuthal symmetry allowing use of a 2-D finite element model to determine the field everywhere in the volume contained by the quadrupole and multi-pole traps. The model includes the magnetic shields, the C-field solenoid, and a number of auxiliary coils that will be described below. These represent the components that determine the magnetic environment of the physics package, except external perturbations, which are small on the scale of interest.

Since we expect the magnetic effect to be determined by field inhomogeneity at the ends of the C-field solenoid and inner shields, we add into the model an auxiliary coil at each end of the multi-pole trap interrogation region to modify the field at these locations. We refer to the coil at the interface between the quadrupole and multi-pole traps as AUX1 ($z \sim 0.43$ m) and that at the other end as AUX2 ($z \sim 0.02$ m).

Figure 4 shows the magnitude of the modeled field along the axis of the physics package. The region from $z = 0$ m to $z = 0.38$ m corresponds to the multi-pole trap electrode region where the microwave interrogation takes place. This figure shows how the field is quite uniform at the lower end ($z = 0$), but not as uniform at the upper end. While improved uniformity will be designed in the next version of this clock, the addition of a trim coil can significantly reduce non-uniformities. The dashed line shows improved uniformity with the application of a current in AUX1.

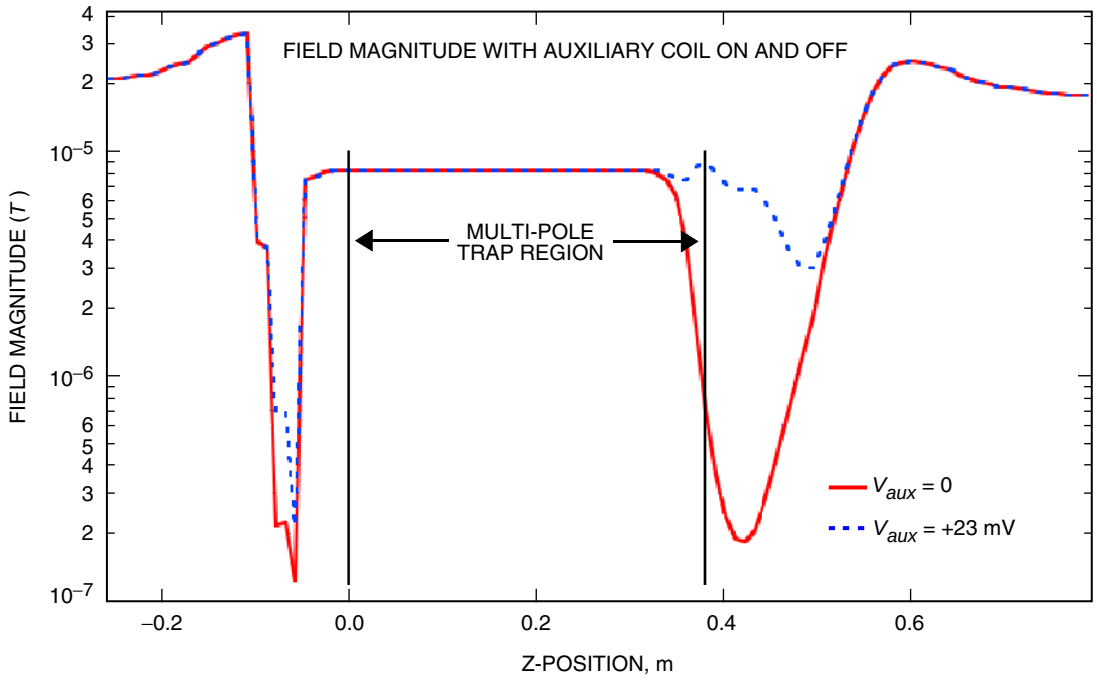

Fig. 4. A plot of the modeled magnetic field magnitude along the axis of the LITS-9 physics package. The solid red line shows the field with only the C-field on. The dashed blue line shows that field modified by the application of the auxiliary coil at the interface between the quadrupole and multi-pole traps, which is also at one end of the C-field solenoid (AUX1). The axial position of 0 m corresponds to the lower end of the C-field solenoid (left side as viewed in Fig. 1), and the region between the vertical black lines corresponds to the multi-pole trap.

The average frequency shift for the second-order Zeeman shift in Hg^+ is

$$\langle \Delta f \rangle = 9.7 \times 10^9 \frac{\mathrm{Hz}}{T^2} \langle B_0^2 \rangle \tag{1}$$

where the average of the field squared is taken over the volume of the trap occupied by the ions. Figure 5 shows how this average frequency shift varies with axial occupation. Each curve represents one setting on the AUX1 coil.

Figure 6 shows the same information, but now keeping the axial occupation fixed at about 95 percent of the trap length and instead varying the radial occupation. As the ion number is changed, space charge repulsion will cause the ion cloud to change its occupation volume in the trap. Each curve in Figs. 5 and 6 can be viewed as qualitatively showing how frequency will vary with ion number for a particular setting of the AUX1 coil.

The axial results (Fig. 5) focus on a small region near the end of the trap. The model implies that, for both directions of ion cloud expansion, we should be able to use AUX1 to change not only the magnitude of the number-dependent shift but its slope as well. This suggests that, in addition to simply improving field homogeneity, we may also reduce the component of the number-dependent shift that depends on trap geometry. The compensated system should yield a very small total ion number-dependent effect.

VI. Modifying the Magnetic Field Environment

To test these predictions, a coil was recently installed on LITS-9 at the AUX1 location. Data were taken before degaussing the magnetic shields (Fig. 7) and after (Fig. 8). The data show good agreement with the model that assumes the cloud expands in the radial direction, but more importantly they demonstrate control over the ion-number frequency shift. The fact that the data remain qualitatively the same before and after shield degaussing indicates that the nature of the field non-uniformity is not due to field non-uniformities in the magnetic shielding. As predicted by the model, the AUX1 coil allows control not only of the offset but also of the slope of the frequency shift versus ion-number curve, thereby making it possible to cancel the two effects and greatly reduce the ion-number dependence.

A. Optimal Coil Setting for Minimal Number Dependence

Figure 9 shows data taken at the optimal AUX1 coil setting (producing best cancellation of number dependence). The absolute setting depends on several factors, including magnetic environment; degaussing history; and trap, C-field, and shield geometry, and it must be redetermined for each situation. The overall shift in these data as determined by a least-squares fit is 0.2(0.3) mHz, or a fractional shift of $\sim 5 \times 10^{-15}$, but within the measurement uncertainty the data are consistent with no shift at all. Even a total 0.2-mHz shift represents an order-of-magnitude improvement over behavior with the AUX1 coil off.

It is essential to point out that cancellation schemes are only as good as they are stable. In this case, long-term data must be taken to verify that the optimal AUX1 coil setting doesn't vary with time. The largest potential contribution to variation would be a change in the magnetic environment. While this might be a concern for a portable standard, the magnetic environment in a metrology laboratory, and specifically that of the Frequency and Timing Test Laboratory at JPL, is quite stable. We anticipate that after degaussing the magnetic shields the coil setting should not need to be changed. Long-term measurements will be made to demonstrate this. Initial measurements show a relative agreement between LITS-9, Universal Coordinated Time at the National Institute for Standards and Technology (UTC-NIST), and Universal Coordinated Time at the U.S. Naval Observatory (UTC-USNO) as measured using Global Positioning System (GPS) time transfer to be better than 2×10^{-16}/day over a 20 day period.

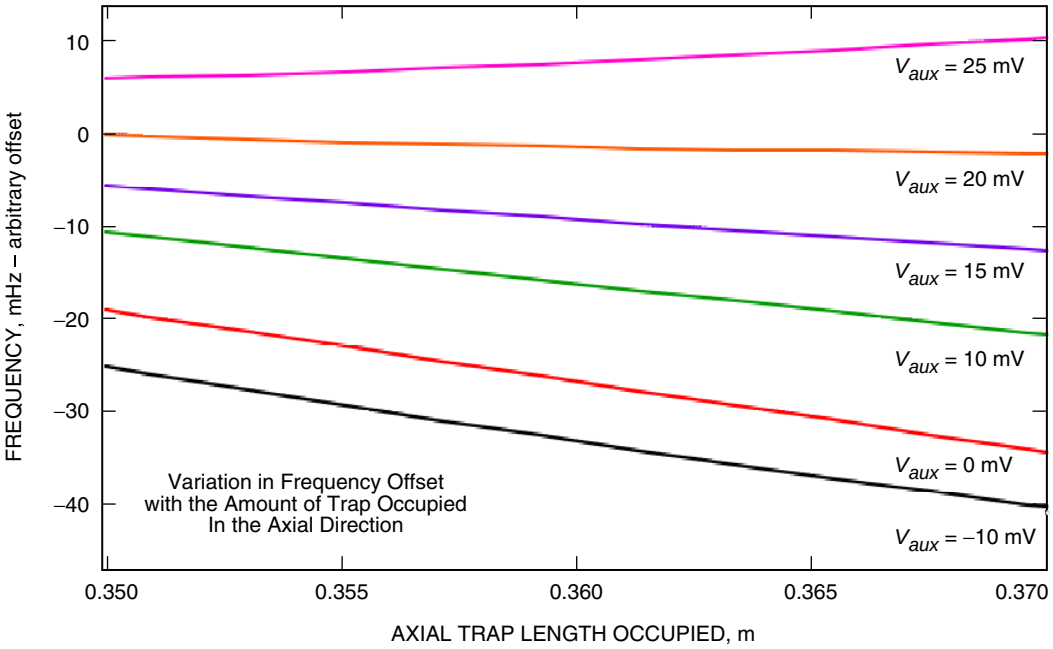

Fig. 5. The average frequency shift modeled for various values of AUX1 current. Each curve plots the average frequency shift as a function of axial occupation (symmetric about the axial center point of the trap) for a single value of current in AUX1. In each case, the shift is relative to a 40.5-GHz transition frequency. For clarity a frequency offset has been removed from each curve.

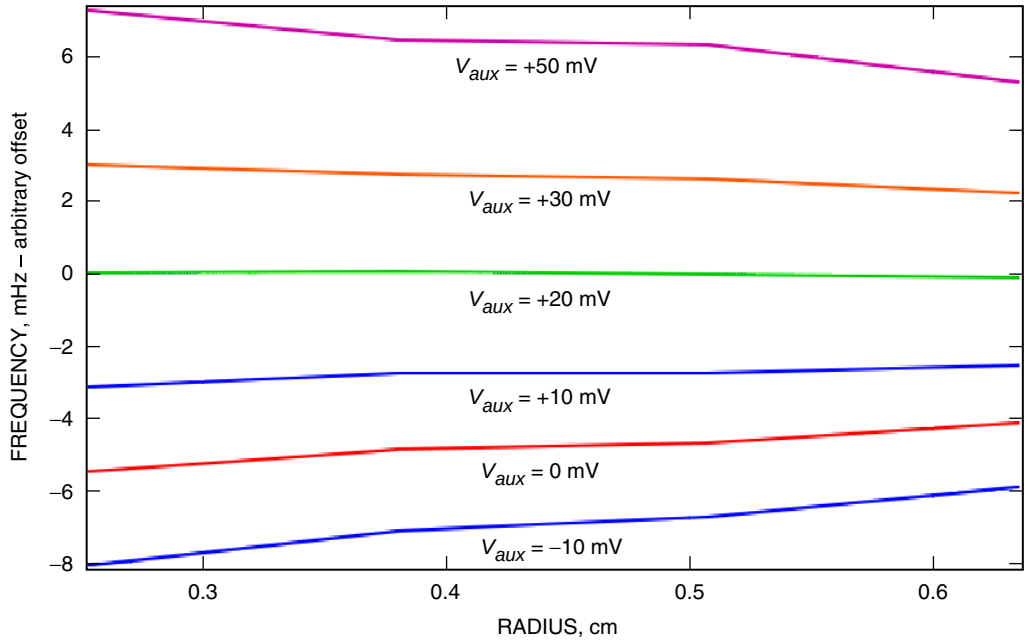

Fig. 6. The average frequency shift modeled for various values of AUX1 current, where each curve now represents a fixed axial occupation and a varying radial occupation. As before, the shift is relative to a 40.5-GHz transition frequency. For clarity an offset between each curve as well as an overall offset have been removed so as to better show the relative changes in slope.

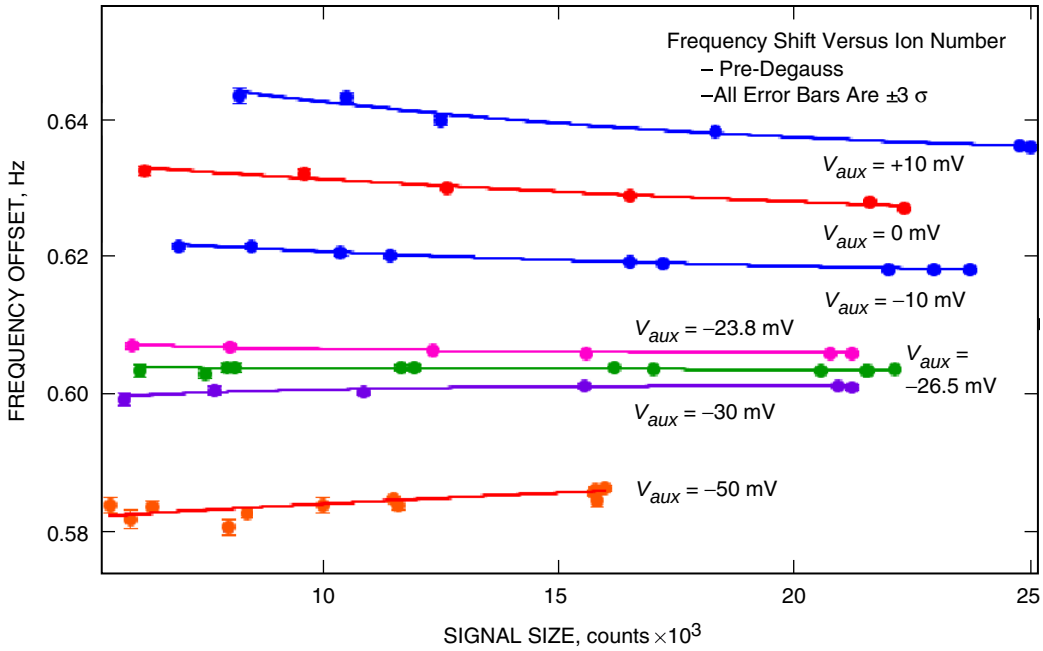

Fig. 7. Measured LITS-9 frequency shifts as a function of ion number (signal size) for various AUX1 coil settings (each curve corresponds to one value of the current in AUX1) before degaussing the magnetic shields. All shifts are relative to the 40.5-GHz Hg^+ clock transition frequency. The data show good agreement with the modeled radial data (Fig. 6).

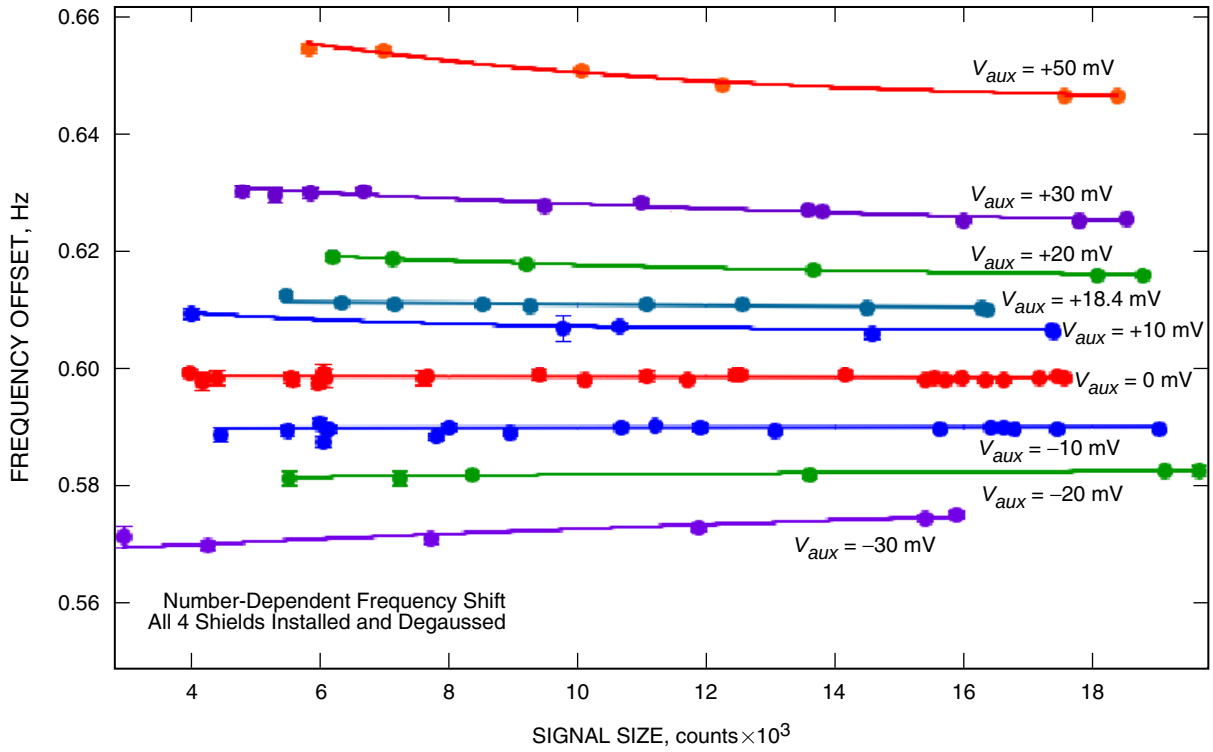

Fig. 8. Measured LITS-9 frequency shifts after the magnetic shields have been degaussed. All shifts are relative to the 40.5-GHz Hg^+ clock transition frequency. The picture remains qualitatively the same, but a different overall offset is introduced.

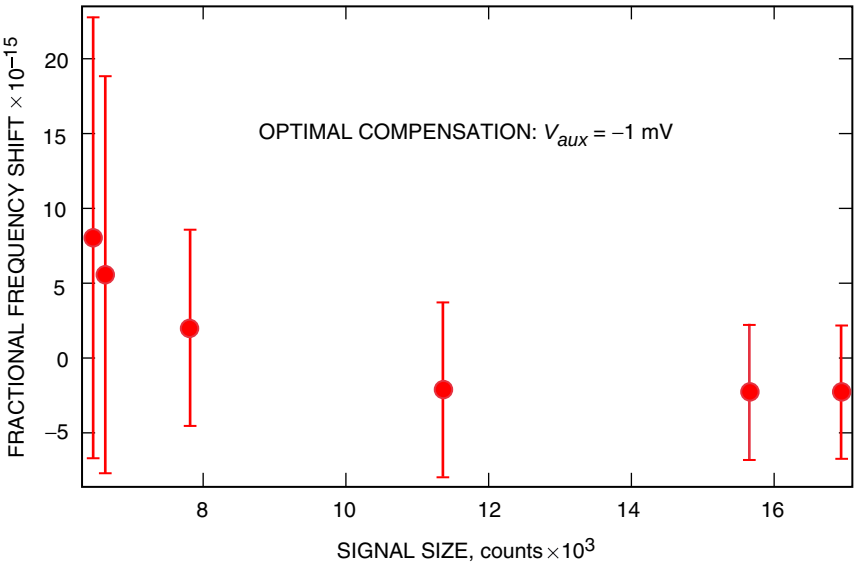

Fig. 9. Frequency shift versus ion number (signal size) data for the optimal AUX1 coil setting (minimal ion-number dependence). Each data point represents 6 hours of data with the error bars representing 3-σ statistical errors.

VII. Estimating the Number-Dependent Second-Order Doppler Shift in the 12-Pole Trap

In addition to estimating optimum cancellation, the model can also indicate the coil setting that gives the best field uniformity. Measuring the ion-number-dependent shift at this setting provides an unmasked estimate of the actual ion-number-dependent second-order Doppler shift alone with no magnetic contribution. Figure 10 shows the second-order Doppler shift using data taken in this way.

As expected, the data show the dramatic improvement in this effect between the quadrupole LITS and the multi-pole LITS [4]. The "compensated" multi-pole data show the potential improvement in stability that might be obtained using AUX1 compared to current multi-pole LITS performance [5]. For instance, if the ion number is stable to 1 percent, then the fractional ion-number-dependent shift in the current multi-pole LITS would be 3×10^{-16}, whereas the same effect in the compensated trap would be $<5 \times 10^{-17}$ (measurement limited by statistical error).

VIII. Neon Buffer Gas: Reducing the Pressure Shift

Untrapped ions in the vicinity of the trap have average energies that are large compared to the trap potential. To trap them, their thermal energy must be reduced. In the LITS, this is accomplished by using an inert buffer gas that, through collisions, remains in thermal equilibrium with the walls of the vacuum chamber. Ions cool by exchanging momentum with buffer-gas atoms during collisions. Previously helium was chosen as the buffer gas for the LITS, and fluctuations in the buffer-gas pressure give the next largest systematic sensitivity after the second-order Doppler shift. Several other candidates for buffer gasses exist, and it has been shown that of these neon has one of the smallest shifts [13,14]. At a 8.9×10^{-9}/torr fractional frequency pressure shift of the Hg^+ clock transition due to neon, this shift is approximately 3× smaller than the helium pressure shift and, because of its larger mass, it cools mercury ions more efficiently, enabling operation at a lower buffer-gas pressure. The neon buffer-gas system now in use in LITS-9 employs a capillary leak instead of the heated quartz leak previously used for helium,

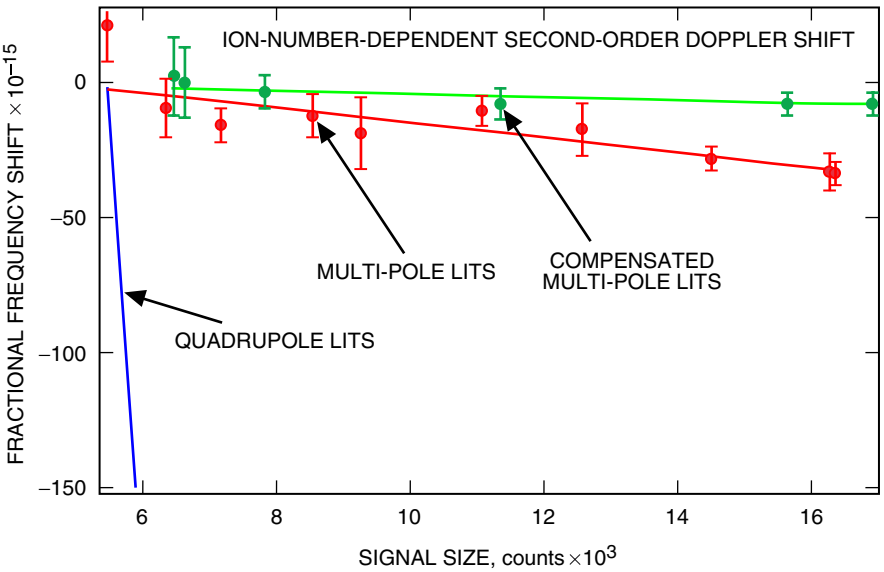

Fig. 10. The ion-number-dependent second-order Doppler shift for the quadrupole LITS (blue), the multi-pole LITS operating with AUX1 set to produce the most uniform field (red), and the multi-pole LITS operating with AUX1 set to produce optimal cancellation of the number-dependent effect (green). The total fractional frequency shift is about 3×10^{-12} for the quadupole LITS, 3×10^{-14} for the multi-pole LITS, and $<5\times10^{-15}$ for the "compensated" multi-pole LITS.

which further improves pressure stability. The helium buffer-gas system limited clock stability at about 2×10^{-16}. With neon, the smaller sensitivity taken together with the lower neon pressure results in about a factor of $6\times$ lower systematic floor due to the pressure shift or $<4\times10^{-17}$. With this change, all known multi-pole LITS sensitivities have been reduced to $<5\times10^{-17}$, resulting in a combined systematic floor of $<6\times10^{-17}$ for LITS-9.

IX. Lamp-Duty Cycle Control: Improved Short-Term Stability

Most of this article has focused on improvements to the multi-pole LITS long-term stability and systematic floor. It is also desirable to improve the short-term stability where possible in order to average down to the systematic floor as fast as possible. The best short-term performance demonstrated in a LITS is $2\times10^{-14}/\tau^{1/2}$ [1,2]. However, this was measured in an older quadrupole LITS that did not have the long-term stability benefits of the multi-pole LITS. Previously the best short-term performance in the multi-pole LITS was about $7\times10^{-14}/\tau^{1/2}$ [16]. The short-term performance of the standard is given by

$$\sigma(\tau) \propto \frac{T_c^{1/2}}{f_0 T_r \mathrm{SNR}\tau^{1/2}} \tag{2}$$

where T_c is the time to execute one complete cycle of the clock, f_0 is the clock frequency, T_r is the interrogation time, SNR is the signal-to-noise ratio of the clock signal, and τ is the averaging time (overall constants of proportionality have been left out). Beyond the simple improvement in SNR, a longer interrogation time will result in better stability at a given averaging time (the longer interrogation time leads to a narrower clock resonance and a larger atomic line Q).

Trapped ion standards, with their long confinement and coherence times, are generally in an ideal position to take advantage of increased interrogation time. However, the LITS uses a discharge lamp for

both state selection and detection. For most discharge lamps, there is an optimal operating temperature that will produce the best SNR (for example, see [9]). Since the lamp is generally switched between a bright (ion loading, state selection, and state detection) and a dim (microwave interrogation) state, it will reach an equilibrium temperature determined by the microwave interrogation time, thereby resulting in a T_r that optimizes SNR. Bimodal operation of the lamp has historically been used to minimize the light shift during microwave interrogation. However, in the multi-pole LITS ions are electromagnetically shuttled from a conventional quadrupole trap used for loading to the multi-pole trap where microwave interrogation takes place. Light leakage from the loading region to the interrogation region is suppressed by a factor of $\sim 10^4$ or more, which is more than the reduction in light between the bright and dim states of the lamp. So in the multi-pole LITS, it is acceptable to have the lamp on during microwave interrogation.

Every discharge lamp is slightly different, but as an example, the lamp currently being used in the multi-pole LITS-9 at JPL has optimal output to pump and detect $^{199}Hg^+$ with a bright/dim duty cycle of about 0.3. The loading, state preparation, and detection take about 4 s. Therefore, this lamp will produce optimal output if the time to shuttle ions to and from the interrogation region (about 1 s) together with the interrogation time is 9.3 s. Different interrogation times dictate a different duty cycle and equilibrium lamp temperature. Small increases in interrogation time can be achieved by externally heating the lamp to give the same equilibrium temperature as in the shorter interrogation time. In fact, this is currently done by heating the lamp enclosure, allowing the interrogation time to be increased to 15 s. The temperature is controlled by a feedback loop to further improve the stability of lamp output. Now, taking advantage of the large light attenuation factor between the two trapping regions, we can increase the total interrogation time by integral multiples of the optimal lamp cycle time without changing the effective lamp output. Figure 11 illustrates this example.

Using this approach to lamp operation, LITS-9 has been operated with a total interrogation time of 30.5 s (the lamp would not be able to support such a low duty cycle if it weren't switched to the bright state in the middle of this interrogation) without loss of SNR. This corresponds to a short-term stability of $6.1 \times 10^{-14}/\tau^{1/2}$, a record for the multi-pole LITS (see Fig. 12). It is notable that this stability is achieved without any impact on long-term systematic effects and that it is obtained using only one of the normally two detection arms. A second arm exists and, if added in with the same SNR, should yield a short-term stability of about $4 \times 10^{-14}/\tau^{1/2}$.

Even longer interrogation times are possible, largely limited by the coherence time of ions in the trap. Figure 13 shows a spectroscopic line using a 65-s interrogation time. The resulting line Q (frequency

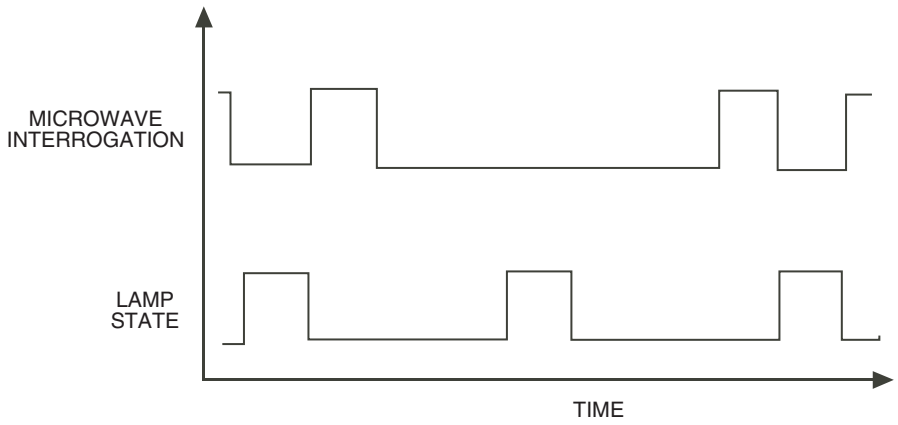

Fig. 11. A timing chart showing the states of microwave interrogation and the discharge lamp as a function of time (not to scale). In this example, two-pulse Ramsey interrogation is used so that the total interrogation time consists of two pulses and a long "free-precession" time in between when the microwave field is turned off. The lamp is shown operating at an optimal duty cycle that includes a bright state during microwave interrogation.

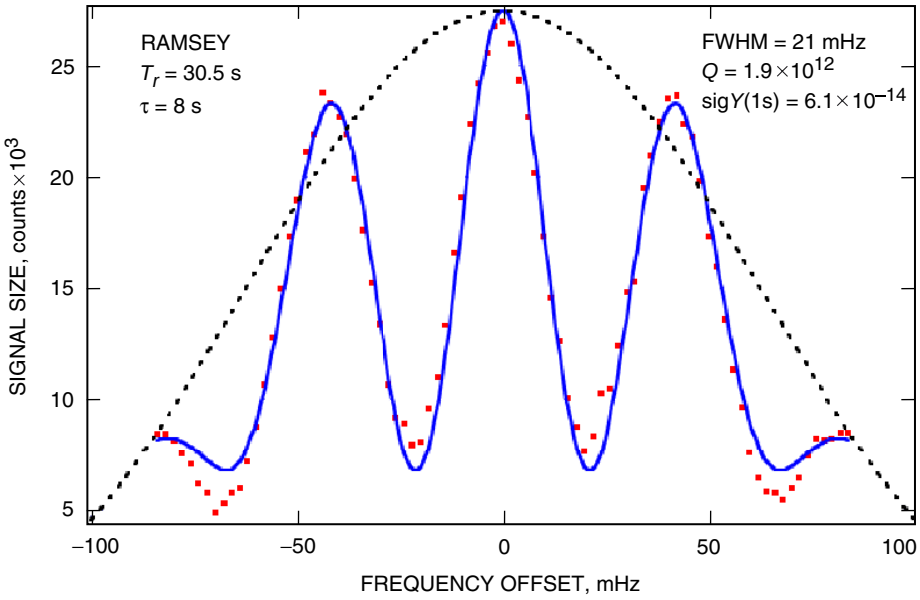

Fig. 12. A spectroscopic line trace of the Hg^+ clock transition using the lamp operating mode described in the text. The Ramsey interrogation method produces fringes as shown with the SNR on the central fringe determining the short-term stability of the clock. For comparison, the dashed line shows the line shape corresponding to a more conventional 6-s interrogation time.

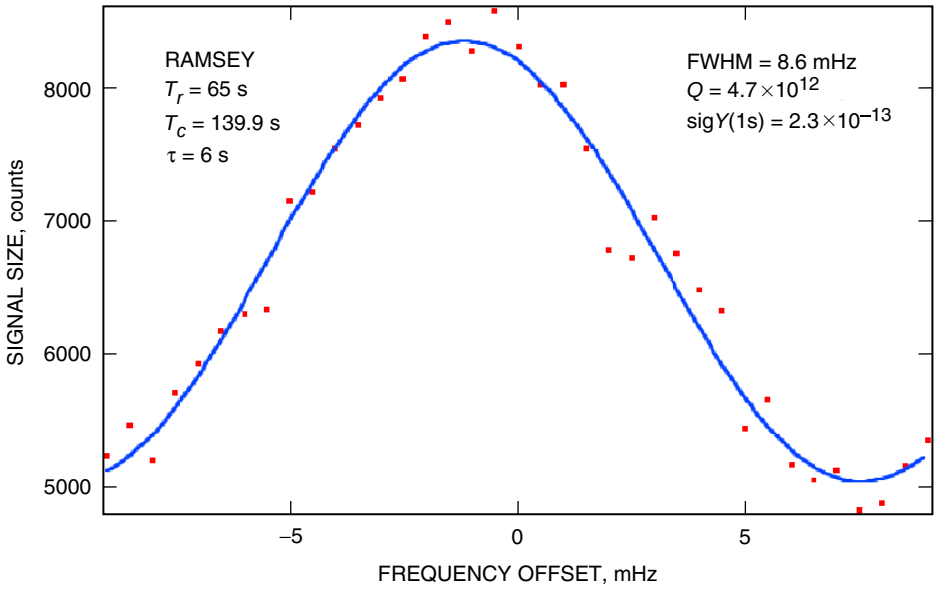

Fig. 13. Spectroscopic line obtained using the new lamp operating scheme with an interrogation time of 65 s. This represents an atomic line Q of 5×10^{12}, the highest ever achieved at room temperature in a microwave transition.

divided by the full-width-at-half-maximum [FWHM] frequency) of 5×10^{12} is the highest ever achieved in a room-temperature microwave frequency standard and within a factor of 2 of the record line Q for the microwave clock transitions measured in laser-cooled Hg^+ [17].

Of course it isn't possible to take advantage of long interrogation times without a local oscillator (LO) that can match the resultant stability for times at least as long as the interrogation time. For field operation, the LITS typically is configured with a quartz LO, and shorter interrogation times of less than 5 s are required to avoid degradation in stability. However, the multi-pole LITS-9 currently is being configured as a laboratory reference and timekeeping standard and can use a hydrogen maser receiver as its LO. The maser receiver has stability as good as or better than LITS-9 for averaging times between 10 and 1000 seconds, thereby allowing closure of the loop anywhere in this range.

X. Conclusions

In this article, we have verified that the source of the "anomalous" second-order Doppler shift is magnetic inhomogeneity and have implemented an auxiliary coil that allows compensation of this effect to less than 5×10^{-17}. We have implemented a capillary leak neon buffer-gas system that reduces sensitivity to pressure fluctuations to less than 4×10^{-17}. With these two largest systematic effects reduced to these levels, the overall systematic floor of the clock is expected to be below 6×10^{-17}. Work is under way to measure the long-term stability of LITS-9 against UTC-USNO, UTC-NIST, and the JPL cesium fountain atomic clock. In addition, we have developed a new discharge lamp operating mode and have demonstrated a signal-to-noise ratio consistent with a short-term stability for the multi-pole LITS of $6.1 \times 10^{-14}/\tau^{1/2}$, making it possible to reach a short-term stability of $4 \times 10^{-14}/\tau^{1/2}$ with two detection arms. Using this lamp operating mode, we also have achieved an atomic line Q of 5×10^{12} in the Hg^+ microwave clock transition that is within a factor of 2 of the best ever achieved for a microwave transition.

References

[1] R. L. Tjoelker, C. Bricker, W. Diener, R. L. Hamell, A. Kirk, P. Kuhnle, L. Maleki, J. D. Prestage, D. Santiago, D. Seidel, D. A. Stowers, R. L. Sydnor, and T. Tucker, "A Mercury Ion Frequency Standard Engineering Prototype for the NASA Deep Space Network," *Proceedings of the 50th Frequency Control Symposium*, Honolulu, Hawaii, pp. 1073–1081, 1996.

[2] G. J. Dick, R. T. Wang, and R. L. Tjoelker, "Cryo-Cooled Sapphire Oscillator with Ultra-High Stability," *Proceedings of the 1998 IEEE International Frequency Control Symposium*, Pasadena, California, pp. 528–533, 1998.

[3] R. L. Tjoelker, J. D. Prestage, and L. Maleki, "Record Frequency Stability with Mercury in a Linear Ion Trap," *Proceedings of the 5th Symposium on Frequency Standards and Metrology*, Woods Hole, Massachusetts, pp. 33–38, 1995.

[4] J. D. Prestage, R. L. Tjoelker, and L. Maleki, "Higher Pole Linear Traps for Atomic Clock Applications," *Proceedings of the 1999 Joint IFCS-EFTF*, Becancon, France, pp. 121–124, 1999.

[5] R. L. Tjoelker, J. D. Prestage, P. A. Koppang, and T. B. Swanson, "Stability Measurements of a JPL Multi-Pole Mercury Trapped Ion Frequency Standard at the USNO," *Proceedings of the 2003 Joint IFCS-EFTF*, Tampa, Florida, pp. 1066–1072, 2003.

[6] R. L. Tjoelker, J. D. Prestage, and L. Maleki, "Improved Timekeeping Using Advanced Trapped-Ion Clocks," *Proceedings of the 31st Annual Precise Time and Time Interval (PTTI) Meeting*, Long Beach, California, pp. 597–604, 1999.

[7] E. A. Burt, J. D. Prestage, and R. L. Tjoelker, "Probing Magnetic Field Effects in 12-Pole Linear Ion Trap Frequency Standards," *Proceedings of the 2002 IEEE IFCS*, New Orleans, Louisiana, pp. 463–468, 2002.

[8] J. D. Prestage, R. L. Tjoelker, and L. Maleki, "Mercury-Ion Clock Based on Linear Multi-Pole Ion Trap," *Procedings of the 2000 IFCS*, Kansas City, Missouri, pp. 706–710, 2000.

[9] R. L. Tjoelker, E. Burt, S. Chung, R. Glaser, R. Hamell, L. Lim, L. Maleki, J. D. Prestage, N. Raouf, T. Radey, C. Sepulveda, G. Sprague, B. Tucker, and B. Young, "Mercury Trapped-Ion Frequency Standard for the Global Positioning System," *Proceedings of the 33rd Annual Precise Time and Time Interval (PTTI) Meeting*, Long Beach, California, pp. 45–54, November 27–29, 2001.

[10] R. L. Tjoelker, E. Burt, S. Chung, R. Glaser, R. Hamell, L. Maleki, J. D. Prestage, N. Raouf, T. Radey, G. Sprague, B. Tucker, and B. Young, "Mercury Trapped Ion Frequency Standard for Space Applications," *Proceedings of the 6th Symposium on Frequency Standards and Metrology*, University of St. Andrews, Fife, Scotland, pp. 609–614, September 9–14, 2001.

[11] J. D. Prestage, S. Chung, T. Le, M. Beach, L. Maleki, and R. L. Tjoelker, "One-Liter Ion Clock: New Capability for Spaceflight Applications," *Proceedings of the 35th Annual Precise Time and Time Interval (PTTI) Meeting*, San Diego, California, pp. 427–433, 2003.

[12] J. D. Prestage, S. Chung, T. Le, L. Lim, and L. Maleki, "Liter Sized Ion Clock with 10^{-15} Stability," *Proceedings of the 2005 Joint IFCS-PTTI*, Vancouver, British Columbia, Canada, pp. 472–476, 2005.

[13] R. L. Tjoelker, S. Chung, W. Diener, A. Kirk, L. Maleki, J. D. Prestage, and B. Young, "Nitrogen Buffer Gas Experiments in Mercury Trapped Ion Frequency Standards," *Proceedings of the 2000 IFCS*, Kansas City, Missouri, pp. 668–671, 2000.

[14] S. K. Chung, J. D. Prestage, R. L. Tjoelker, and L. Maleki, "Buffer Gas Experiments in Mercury (Hg^+) Ion Clock," *Proceedings of the 2004 IFCS*, Montreal, Canada, pp. 130–133, 2004.

[15] W. M. Itano, L. L. Lewis, and D. J. Wineland, "Shift of $^2S_{1/2}$ Hyperfine Splittings due to Blackbody Radiation," *Phys. Rev. A*, vol. 25, pp. 1233–1235, 1982.

[16] J. D. Prestage, R. L. Tjoelker, and L. Maleki, "Recent Developments in Microwave Ion Clocks," *Topics in Applied Physics*, vol. 79, pp. 195–211, 2001.

[17] D. J. Berkeland, J. D. Miller, J. C. Bergquist, W. M. Itano, and D. J. Wineland, "Laser-Cooled Mercury Ion Frequency Standard," *Phys. Rev. Lett.*, vol. 80, pp. 2089–2092, 1998.